CCS Chemistry

RESEARCH ARTICLE

Received: Oct. 25, 2023 | Accepted: Dec. 8, 2023 | Published: Jan. 10, 2024

Asymmetric Autotandem Palladium Catalysis for α,β-Unsaturated Lactones: Merging Olefin and Ester Hydrogenation

Lei Sun[1†], Han Wang[1†], Die Bai[2], Chang-Bin Yu[1], Bo Wu[1], Rong-Zhen Liao[2*] & Yong-Gui Zhou[1*]

[1]State Key Laboratory of Catalysis, Dalian Institute of Chemical Physics, Chinese Academy of Sciences, Dalian 116023, Liaoning, [2]School of Chemistry and Chemical Engineering, Huazhong University of Science and Technology, Wuhan 430074, Hubei

**Corresponding authors: ygzhou@dicp.ac.cn; rongzhen@hust.edu.cn; †*L. Sun and H. Wang contributed equally to this work.

Cite this: *CCS Chem*. **2024**, 6, 1987–1999
DOI: 10.31635/ccschem.023.202303564

Autotandem catalysis (ATC) is fascinating since a single catalyst can promote tandem reactions involving two or more mechanisms in a single reactor and is a highly desirable approach to realize multifarious transformations in organic synthetic chemistry. Herein, a palladium-catalyzed asymmetric autotandem hydrogenation of α,β-unsaturated lactones is disclosed, providing chiral saturated alcohols. In this reaction, the C=C bond in α,β-unsaturated lactones was first hydrogenated to give the dihydrocoumarins with high enantioselectivity, followed by hydrogenation of the ester group with the same catalytic system. Notably, after decreasing the reaction temperature, hydrogenation of the single C=C bond proceeded smoothly, delivering the dihydrocoumarin products with high yield and enantioselectivity. Control experiments and density functional theory calculations were carried out to elucidate the cause of this unusual asymmetric autotandem hydrogenation. Notably, the homogeneous palladium catalyst was successfully applied in the hydrogenation of esters under neutral conditions.

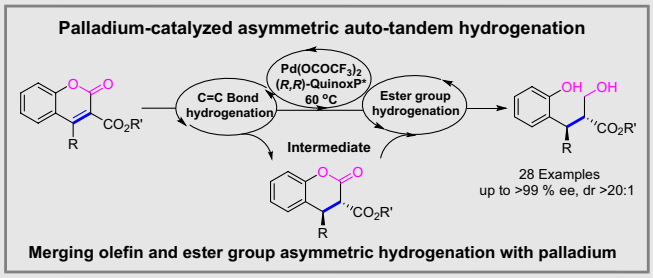

Keywords: **autotandem catalysis, asymmetric hydrogenation, chiral dihydrocoumarins, hydrogenation of esters, α,β-unsaturated esters**

Introduction

Tandem reactions are frequently utilized in organic synthesis due to their high atom and step economy.[1-3] In fact, since mechanistically distinct transformations in tandem reactions are usually encountered, multiple catalysts are chosen to realize the desired reactions. Autotandem catalysis (ATC), originally defined by Fogg and dos Santos,[4] has been extensively studied over the past decades.[4-6] In ATC reactions, a single catalyst sequentially catalyzes two or more chemical transformations with different mechanisms in a single reactor. Compared to tandem reactions, ATC reactions feature outstanding advantages, which not only are thermodynamically

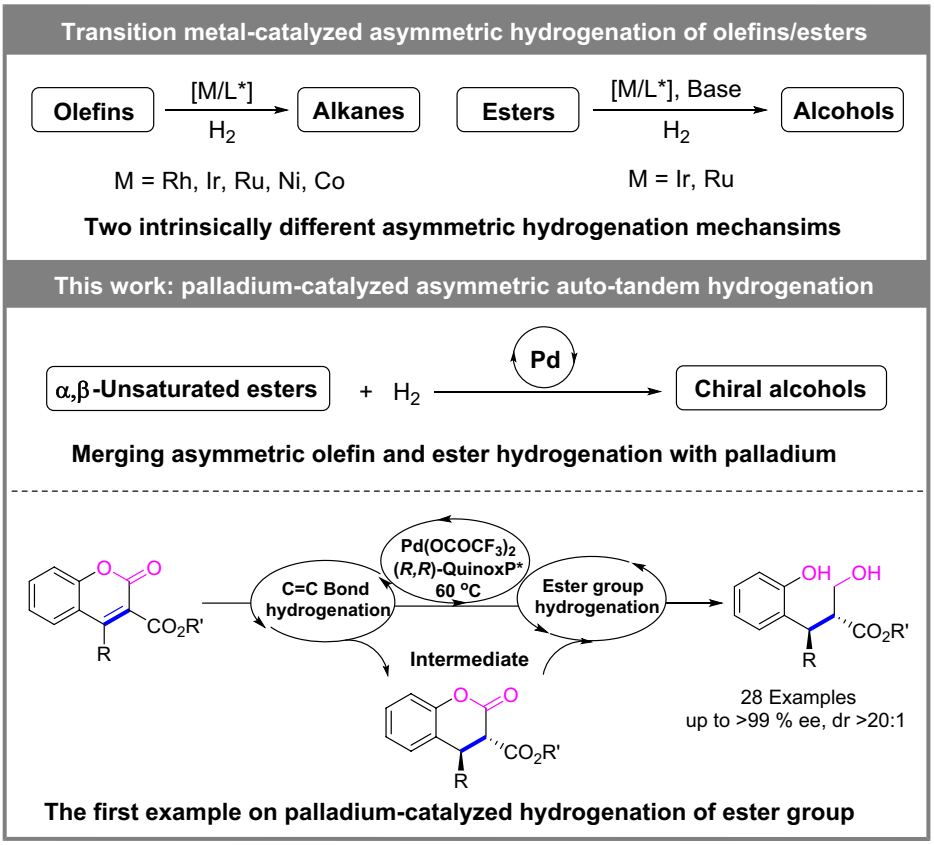

Scheme 1 | *Palladium-catalyzed asymmetric autotandem hydrogenation of α,β-unsaturated lactones.*

favourable by coupling the multiple catalytic cycles, but also make full use of the multiple functions of a catalyst. Therefore, the development of ATC reactions is extremely attractive. Nonetheless, the ATC reaction still involves great challenges because it is difficult to identify the optimum conditions that suit the multiple reactions. Although impressive progress has recently been achieved with respect to ATC reactions, the relevant asymmetric versions lack sufficient study.[7-9]

Transition-metal-catalyzed asymmetric hydrogenation of olefins to optically active alkanes[10-15] and hydrogenation of esters to chiral alcohols[16-22] have been recognized as well-exploited areas in asymmetric hydrogenation (Scheme 1). However, due to their intrinsic differences, the transition-metal catalytic systems for asymmetric hydrogenation of olefins are different from those for the hydrogenation of esters. To date, a plethora of transition-metal catalysts have enabled asymmetric hydrogenation of olefins.[10-15] Asymmetric hydrogenation of esters have performed successfully with iridium or ruthenium catalysts under the basic condition (Scheme 1).[16-22] Notably, transition-metal-catalyzed asymmetric hydrogenation of α,β-unsaturated esters commonly occur at the C=C bond, and the relatively inert ester can be retained.[23-33] The catalysts that show superior performance in the asymmetric hydrogenation of olefins, conversely, are inert for ester hydrogenation and vice versa. To date, hydrogenation of both olefin and ester with the same catalytic system has been less exploited. As a result, asymmetric hydrogenation of α,β-unsaturated esters to the chiral saturated alcohols still requires a two-step process.

In our continuous efforts in homogeneous palladium-catalyzed asymmetric hydrogenation,[34-39] we envisage applying the palladium catalytic system to the asymmetric hydrogenation of more challenging tetrasubstituted olefins,[40-46] the disubstituted α,β-unsaturated lactones. During the exploration of palladium-catalyzed asymmetric hydrogenation of α,β-unsaturated lactone. both C=C bond and ester group hydrogenated product was observed, and we reasoned that this reaction was an asymmetric ATC. Herein, we describe the palladium-catalyzed auto-tandem asymmetric hydrogenation of the C=C bond and ester group of α,β-unsaturated lactones with high reactivity and enantioselectivity (Scheme 1). By decreasing the reaction temperature, the hydrogenation of the single C=C bond proceed smoothly, delivering the dihydrocoumarin products with high enantioselectivity. Notably, this is the first homogeneous palladium-catalyzed hydrogenation of ester group under neutral conditions. The control experiments and density functional theory (DFT)

DOI: 10.31635/ccschem.023.202303564
Citation: *CCS Chem.* **2024**, 6, 1987–1999
Link to VoR: https://doi.org/10.31635/ccschem.023.202303564

calculations provide important insight into the origin of this unusual asymmetric autotandem hydrogenation.

Experimental Methods

General procedure for palladium-catalyzed asymmetric hydrogenation of C=C and esters

$Pd(OCOCF_3)_2$ (0.01 mmol, 3.2 mg, 5 mol %), ligand (*R,R*)-QuinoxP* (0.012 mmol, 4.0 mg, 6 mol %), and degassed anhydrous acetone (1.0 mL) were placed in a dried Schlenk tube under nitrogen atmosphere. The mixture was stirred at room temperature for 1 h. The solvent was removed under vacuum to give the catalyst. This catalyst was placed in a glove box filled with nitrogen and dissolved in 2,2,2-trifluoroethanol (TFE, 1.0 mL). To the mixture of α,β-unsaturated lactones **1** (0.2 mmol) and TFE (2.0 mL) was added this catalyst solution, and then the mixture was transferred to an autoclave, which was charged with hydrogen gas to 600 psi (41 bar). The reaction mixture was stirred at 60 °C for 36–40 h. After cooling to room temperature and the release of the hydrogen gas, the autoclave was opened, and the volatiles were removed under the reduced pressure. Then, the residue was purified by column chromatography on silica gel using hexanes/ethyl acetate (10:1–2:1) as eluent to give the chiral reductive products **2**. The enantiomeric excesses were determined by chiral high-performance liquid chromatography (HPLC) with chiral column. Racemates of reductive products **2** were prepared by reduction of the α,β-unsaturated lactones **1** with the achiral ligand 1,2-bis(dicyclohexylphosphino)ethane.

General procedure for palladium-catalyzed asymmetric hydrogenation of C=C bonds

$Pd(OCOCF_3)_2$ (0.002 mmol, 0.7 mg, 1 mol %), ligand (*R,R*)-QuinoxP* (0.0024 mmol, 0.8 mg, 1.2 mol %), and degassed anhydrous acetone (1.0 mL) were placed in a dried Schlenk tube under nitrogen atmosphere. The mixture was stirred at room temperature for 1 h. The solvent was removed under vacuum to give the catalyst. This catalyst was placed in a glove box filled with nitrogen and dissolved in TFE (1.0 mL). To the mixture of coumarins **1** (0.2 mmol) and TFE (2.0 mL) was added the catalyst solution, and the mixture was transferred to an autoclave, which was charged with hydrogen gas to 400 psi (27.5 bar). The reaction mixture was stirred at 30 °C for 24 h. After release of the hydrogen gas, the autoclave was opened, and the volatiles were removed under the reduced pressure. Then the residue was purified by column chromatography on silica gel using hexanes/ethyl acetate (5:1) as eluent to give the pure reductive products **3**. Racemates of **3** were prepared by reduction of the α,β-unsaturated lactones **1** with the achiral ligand 1,2-bis(dicyclohexylphosphino)ethane.

Results and Discussion

At the beginning of the investigation, α,β-unsaturated lactone **1a** was chosen as a model substrate for palladium-catalyzed asymmetric autotandem hydrogenation. To our delight, both C=C bond and ester group hydrogenated product **2a** were obtained with 96% isolated yield, >20:1 diastereoselectivity, and >99% ee in TFE at 60 °C (Table 1, entry 1). Next, the effect of solvents on reactivity and stereoselectivity was examined. Asymmetric autotandem hydrogenation in hexafluoroisopropanol (HFIP) resulted in slight erosion of reactivity (entry 2). No reaction took place in dichloromethane, toluene, tetrahydrofuran, or ethyl acetate (entries 3–6).

Next, a series of chiral electron-donating bisphosphine ligands were investigated (entries 7–9). None of them showed better performance than the (*R,R*)-QuinoxP*. Regrettably, (*R*)-SegPhos (**L5**) showed low reactivity (entry 10). By decreasing the reaction time from 36 h to 24 h, the target product was obtained with 94% yield and >99% ee, and the olefin hydrogenation product **3a** was observed in 6% yield (entry 11). Thus, the optimized conditions for asymmetric autotandem hydrogenation were established: $Pd(OCOCF_3)_2$/(*R,R*)-QuinoxP*, TFE, and hydrogen (600 psi) at 60 °C for 36 h.

Based on the optimum condition of the above asymmetric ATC hydrogenation, we further decreased the temperature to 30 °C as well as catalyst loading to 1 mol %. To our delight, only olefin hydrogenation product **3a** was obtained with 98% yield and 97% ee in 24 h (entry 12). Notably, owing to the existence of classical keto/enol tautomerization, the product was formed as a mixture of *cis* and *trans* diastereomers. Clean nuclear magnetic resonance (NMR) spectra and HPLC spectra were not obtained. Fortunately, the in situ alkylation with allyl bromide provided the stable compound **3a′** with high diastereoselectivity (>20:1 dr).[a] Consequently, the optimized condition for C=C bond asymmetric hydrogenation of α,β-unsaturated lactones was also established as follows: $Pd(OCOCF_3)_2$/(*R,R*)-QuinoxP*, TFE, and hydrogen gas (400 psi) at 30 °C for 24 h.

To prove the generality of the method, the substrate generality of α,β-unsaturated lactones was explored. First, asymmetric ATC hydrogenation of 4-alkyl substituted 3-alkoxy-carbonylcoumarins was carried out, and the results are presented in Scheme 2. Then different alcohols were obtained in good yield and >99% ee, no matter whether the C4 position was alkyl (**2b–2d**) or aryl (**2o–2q**). Then, the steric effect on the phenyl of the α,β-unsaturated lactones was further examined. Substrate **1g** bearing a methyl substituent on the C8 position performed smoothly to afford the corresponding product **2g** in >99% ee and moderate yield. Products **2e** and **2f** with methyl substituents on the C6 and C7 positions were obtained with up to 95% yield and >99% ee. Moreover,

DOI: 10.31635/ccschem.023.202303564
Citation: *CCS Chem.* **2024**, 6, 1987–1999
Link to VoR: https://doi.org/10.31635/ccschem.023.202303564

Table 1 | *Condition Optimization*[a]

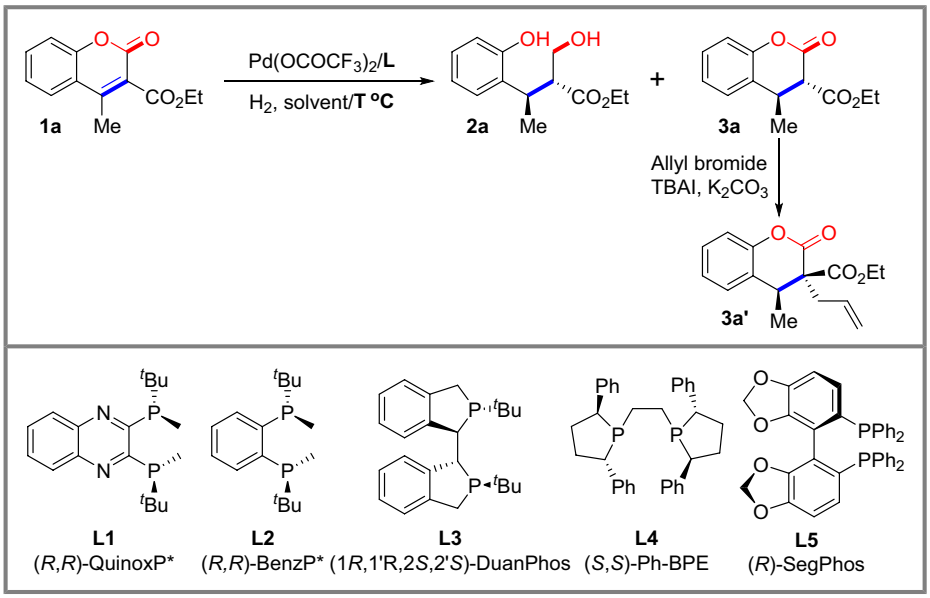

			2a		3a′	
Entry	Solvent	**L**/T (°C)	Yield (%)[b]	ee (%)[c]	Yield (%)[b]	ee (%)[d]
1	TFE	**L1**/60	>95[e]	>99	<5	—
2	HFIP	**L1**/60	94	99	5	—
3	DCM	**L1**/60	<5	—	<5	—
4	Toluene	**L1**/60	<5	—	<5	—
5	THF	**L1**/60	<5	—	<5	—
6	EA	**L1**/60	<5	—	<5	—
7	TFE	**L2**/60	>95	95	<5	—
8	TFE	**L3**/60	94	91	6	—
9	TFE	**L4**/60	94	89	6	—
10	TFE	**L5**/60	<5	—	<5	—
11[f]	TFE	**L1**/60	94	>99	6	—
12[g]	TFE	**L1**/30	<5	—	98	97

[a] Reaction conditions: **1a** (0.20 mmol), $Pd(OCOCF_3)_2$ (5.0 mol %), ligand (6.0 mol %), H_2 (600 psi), solvent (2.0 mL), 36 h.
[b] Determined by ^1H NMR using dibromomethane as internal standard, and all the products have >20:1 dr.
[c] Determined by HPLC.
[d] The enantiomeric excess of **3a** was determined by HPLC after being protected by allyl bromide.
[e] Isolated yield is 96%.
[f] Reaction was conducted for 24 h.
[g] **1a** (0.20 mmol), $Pd(OCOCF_3)_2$ (1.0 mol %), ligand (1.2 mol %), H_2 (400 psi), solvent (2.0 mL), 24 h.
DCM, dichloromethane; THF, tetrahydrofuran; EA, ethyl acetate.

substrates with different alkyl groups at the C4 position were examined. The hydrogenation performed smoothly when the substituents on the C4 position were ethyl, *n*-propyl, *n*-butyl, and cyclopropyl (**2i–2l**). Due to the steric effect, 4-cyclohexyl and 4-benzyl substrates showed slight erosion of reactivities with high enantioselectivities (**2m**, **2n**). Sequentially, changing the ester to an amide group resulted in 88% yield and >99% ee (**2r**). Unfortunately, the substituents on the *ortho*-position of the aryl group showed an apparent steric effect and led to obvious erosion of both reactivity and enantioselectivity (**2s**), while the substituents at the *para*- and *meta*-position of the aryl group scarcely influenced the yields and enantioselectivities (**2t**, **2u**).

Furthermore, the electronic effect of the substituents on aryl was investigated, and both electron-donating and electron-withdrawing substituents afforded 98% yield and >99% enantioselectivities (**2v–2x**). Notably, free hydroxyl and protected hydroxyl groups achieved excellent enantioselectivities and yields (**2y**, **2z**). When the aryl on the C4 position was the 2-naphthyl group, the desired product **2aa** was obtained with 97% yield and >99% ee. The substrate **1ac** bearing a thiophene group delivered the desired product **2ac** with >99% ee in low 15% yield,

DOI: 10.31635/ccschem.023.202303564
Citation: *CCS Chem.* **2024**, 6, 1987–1999
Link to VoR: https://doi.org/10.31635/ccschem.023.202303564

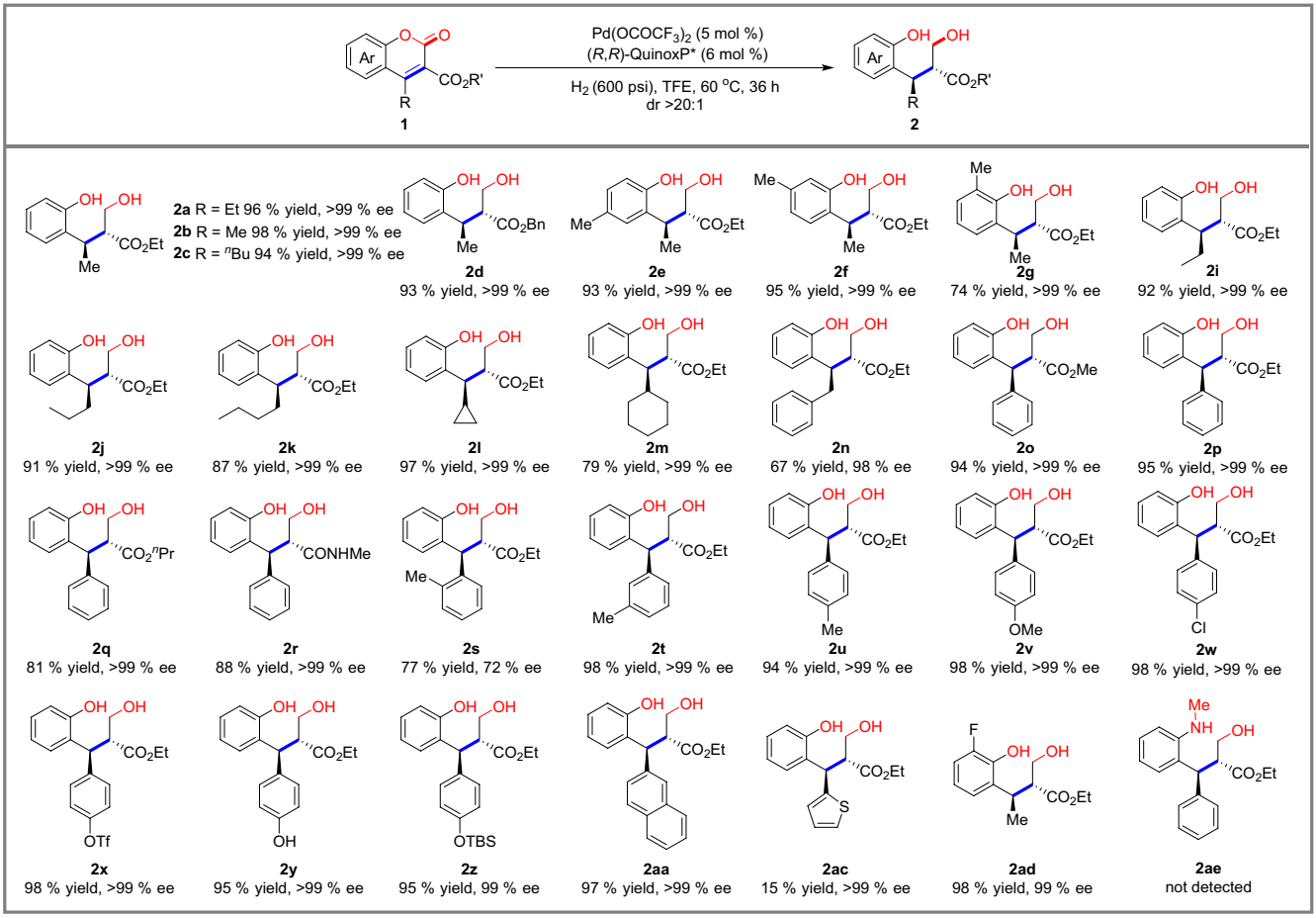

Scheme 2 | *Substrates scope: α,β-unsaturated lactones (AH of C=C and ester).*

which might be ascribed to the poison effect of thiophene. The product **2ad** with a fluoro atom in the C8 position was hydrogenated with 98% yield and 99% ee. Unfortunately, the ATC reaction of 4-phenyl 3-(ethoxycarbonyl)quinolin-2-ones (**1ae**) did not take place.

Chiral dihydrocoumarins have been served as a class of crucial structural motifs in natural products and biologically active molecules. Asymmetric reduction of chromen-2-ones is one of the most straightforward approaches to access the chiral dihydrocoumarins. Rhodium-, ruthenium-, and iridium-catalyzed asymmetric hydrogenation of chromen-2-ones, as well as chiral and regenerable nicotinamide adenine dinucleotide phosphate (NAD(P)H) model-enabled catalytic biomimetic asymmetric reduction of chromen-2-ones, have been developed that yield optically active dihydrocoumarins in excellent enantioselectivities.[45,47–50] Given the importance of chiral dihydrocoumarins and the fact that exploration of new transition-metal catalytic systems would facilitate the development of asymmetric hydrogenation of chromen-2-ones, we turned our attention to palladium-catalyzed asymmetric hydrogenation of chromen-2-ones and only C=C bonds was hydrogenated (Scheme 3). The hydrogenation products (**3a–3n**) were in situ allylated with allyl bromide in consideration of the tendency to racemize the α-position of ester. Firstly, the different esters were examined under the optimized condition, good yields, and excellent enantioselectivities were obtained. In addition, the substrates with methyl substituent on the C6 (**3e′**), C7 (**3f′**), and C8 (**3g′**) positions of coumarins were examined, and they showed no diminution of reactivity or enantioselectivity. Moreover, when we changed the phenyl ring of α,β-unsaturated lactone to naphthyl ring, 88% yield and 96% ee were observed. Eventually, the steric effects of the substitutions on the C4 position were explored. Various alkyl substituents, such as ethyl, *n*-propyl, *n*-butyl, cyclopropyl, cyclohexyl, and benzyl (**3i′–3n′**), achieved excellent reactivities and enantioselectivities.

Following the delightful results of the C=C bond hydrogenation of alkyl-substituted α,β-unsaturated lactones, we turned our attention to the aryl-substituted α,β-unsaturated lactones. Good yields and excellent enantioselectivities were obtained when the R′ group was methyl, ethyl, or propyl (**3o–3q**). Next, changing the ester group to an amide group resulted in 92% yield and >99% ee (**3r**). Furthermore, the steric and electronic effects of the substituents on aryl were investigated. The

DOI: 10.31635/ccschem.023.202303564
Citation: *CCS Chem.* **2024**, 6, 1987–1999
Link to VoR: https://doi.org/10.31635/ccschem.023.202303564

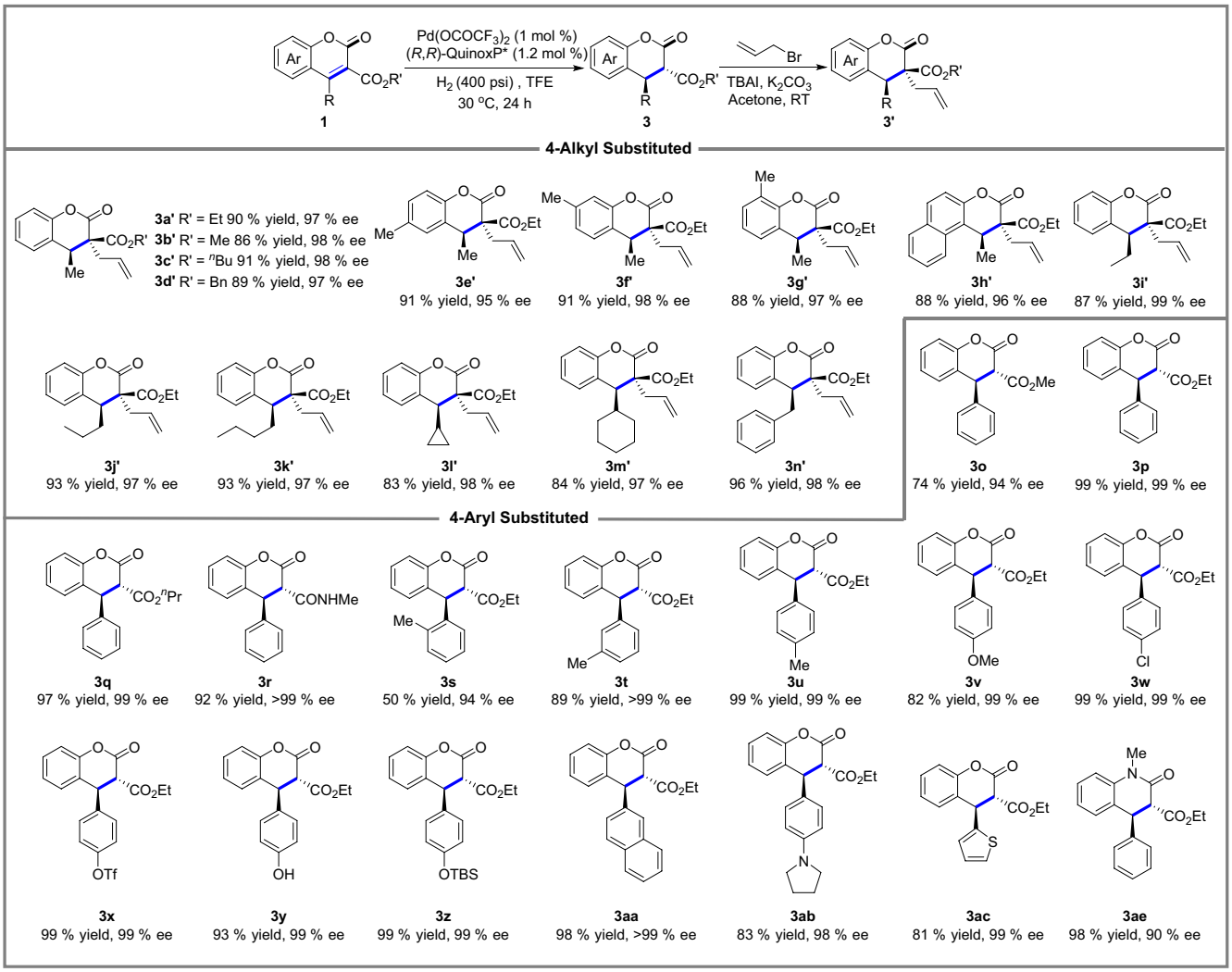

Scheme 3 | *Substrate scope: α,β-unsaturated lactones (AH of C=C only).*

substituents on *para*- and *meta*-position of the aryl group marginally influenced the yields and enantioselectivities (**3t**, **3u**), but the substituents on *ortho*-position of the aryl group showed an obvious steric effect, leading to crucial erosion of reactivity (**3s**). In contrast, either electron-donating (**3v**) or electron-withdrawing (**3w**, **3x**) substituents achieved excellent enantio-selectivities. An erosion of yield was observed in the presence of a free hydroxyl group, while excellent yield and enantioselectivity were obtained when the hydroxyl group was protected by *t*-butyldimethylsilyl. For 2-naphthyl substituted **3aa** achieved 98% yield and >99% ee. For **3ab** and **3ac** containing the pyrrolidine and thiophene skeleton, excellent enantioselectivity was achieved albeit with slightly lower yield. Eventually, **3ae** containing lactam was achieved with 98% yield and 90% ee under 80 °C.

In order to demonstrate the utility of this reaction, we carried out the palladium-catalyzed asymmetric autotandem hydrogenation at the gram scale as well as further transformations (Scheme 4). To our delight, the target product **2p** (the absolute configuration was determined by X-ray, for detail, see Supporting Information Figure S1) was obtained in 93% yield, >99% ee, and >20:1 dr without any loss of reactivity and enantioselectivity. Furthermore, the hydroxyl and ester groups were attractive functional groups for further transformations. The intramolecular transesterification was performed in the presence of *p*-toluenesulfonic acid with 96% yield. On the other hand, the Mitsunobu reaction was a proper approach to achieve ether **5**. Reduction of **2p** with lithium aluminum hydride afforded the chiral triol, which was further protected by benzoyl chloride for HPLC analysis. For all of the above transformations, no loss of optical purity was observed.

To gain further insight into the mechanism, a series of control experiments was conducted (Scheme 5). First, the reaction proceeded under the standard conditions for 8 h. As a result, C=C bond hydrogenated product **3p** and both C=C and ester group hydrogenated product **2p** were obtained in 46% and 23% yields, respectively. To

DOI: 10.31635/ccschem.023.202303564
Citation: *CCS Chem.* **2024**, 6, 1987–1999
Link to VoR: https://doi.org/10.31635/ccschem.023.202303564

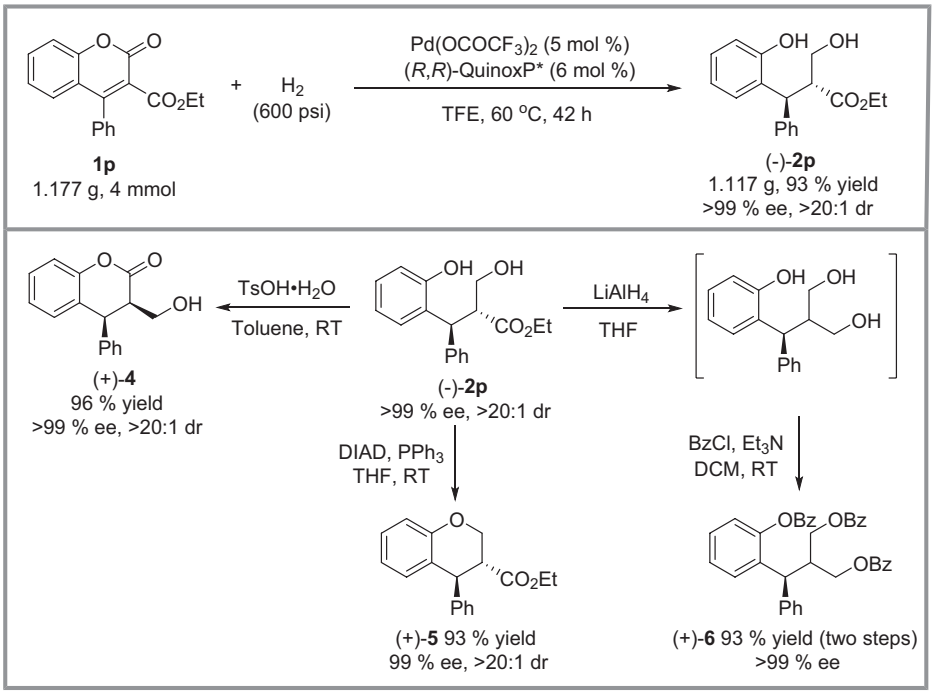

Scheme 4 | *Experiment at gram scale and product derivatization.*

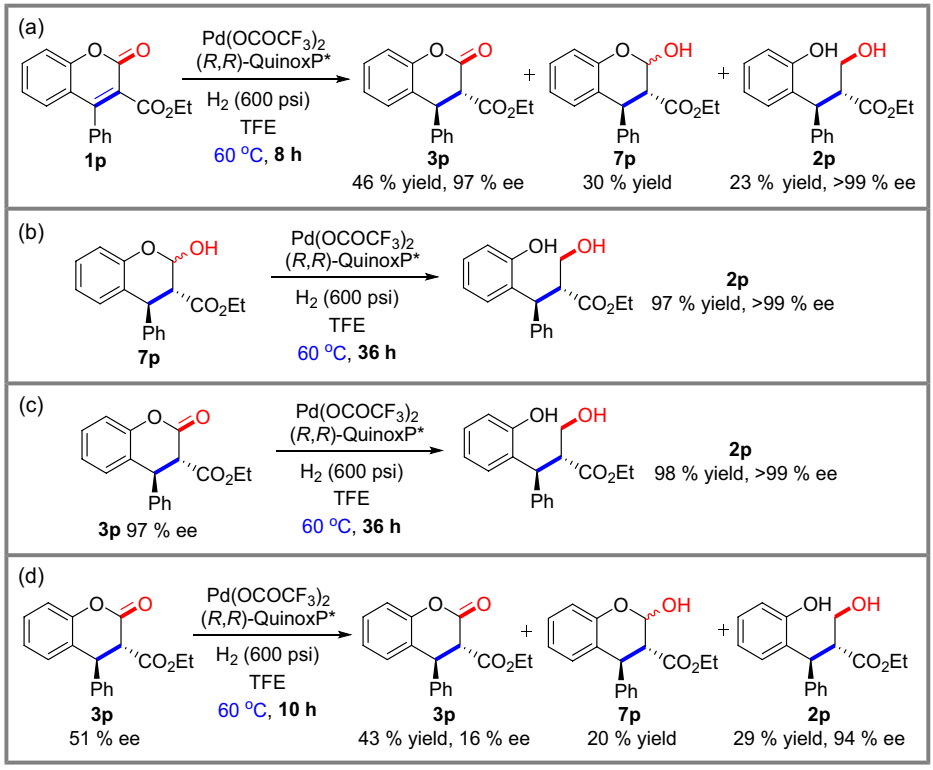

Scheme 5 | *Mechanistic studies.*

DOI: 10.31635/ccschem.023.202303564
Citation: *CCS Chem.* **2024**, 6, 1987–1999
Link to VoR: https://doi.org/10.31635/ccschem.023.202303564

our surprise, hemiacetal **7p** was isolated in 30% yield and was also characterized (Scheme 5a), suggesting that the hemiacetal **7p** might be a key intermediate of hydrogenation of the ester group. Furthermore, the treatment of the hemiacetal **7p** under the standard conditions afforded the target product **2p** with the same 97% yield and >99% ee (Scheme 5b), further demonstrating that the hemiacetal **7p** was an intermediate of ester group hydrogenation.

The target product **2p** with >99% ee was transformed from **3p** with 97% ee, which indicated an enantioselectivity promotion during the hydrogenation process of ester. We assumed that the hydrogenation of ester involved a kinetic resolution process. The enantiomeric ratio of **3p** was 98.5 (*S*,*S*)/1.5 (*R*,*R*) (Scheme 5c). Only the favoured (*S*,*S*)-isomer was able to further the hydrogenation of ester, which might result in enantioselectivity promotion. To prove the above hypothesis, we carried out the asymmetric hydrogenation using **3p** with 51% ee as the starting material, and it shut down the hydrogenation after 10 hours. To our delight, the 43% starting material **3p** remained with decreased 16% ee, and the target product **2p** was obtained in 29% yield and increased 94% ee (Scheme 5d). The obvious ee decrease of recovered substrate **3p** indicated that the asymmetric hydrogenation of the ester group involved a process of kinetic resolution, which resulted in enantioselectivity promotion (Supporting Information Figure S2).

To further investigate the ATC reaction, we analyzed the reaction mixture over time. As a result, an ATC process could be clearly observed, as shown in Figure 1. The starting material **1p** was rapidly consumed over the first two hours. At the same time, the C=C bond hydrogenation product **3p** formed. In contrast, the hemiacetal **7p** and both C=C bond and ester group hydrogenation product **2p** were not observed in the first 2 h. As the reaction proceeded, the C=C bond hydrogenation product **3p** was consumed slowly, and the ATC hydrogenation product **2p** was generated. Notably, the hemiacetal intermediate **7p** was formed during 2–10 h and then was consumed during the last 12 h. The hemiacetal species **7p** remained at a lower concentration, which suggests that **7p** is the key intermediate of the ATC reaction.

To further provide strong evidence for the ATC hydrogenation mechanism, we carried out DFT calculations[b] of all possible hydrogenation reaction pathways. The simplified Gibbs energy diagrams for the three sequential hydrogenation reactions are shown in Figures 2–4 (for details, see Supporting Information Figures S3–S8 and Table S1).

The first stage of the reaction is the hydrogen activation by the Pd(OCOCF$_3$)$_2$/(*R*,*R*)-QuinoxP* catalyst (labeled as Cat) via a heterolytic cleavage mechanism, associated with a barrier of only 14.0 kcal/mol (Supporting Information Figure S3). Then, the generated Pd-H species[40] was used to react with substrate **1o**. In this case, three possible attacks by the Pd-H species can be envisioned, namely C1 of the C=C double bond, C2 of the lactone C=O double bond, and C3 of the terminal ester C=O double bond. Each attack generated an *R* or *S*

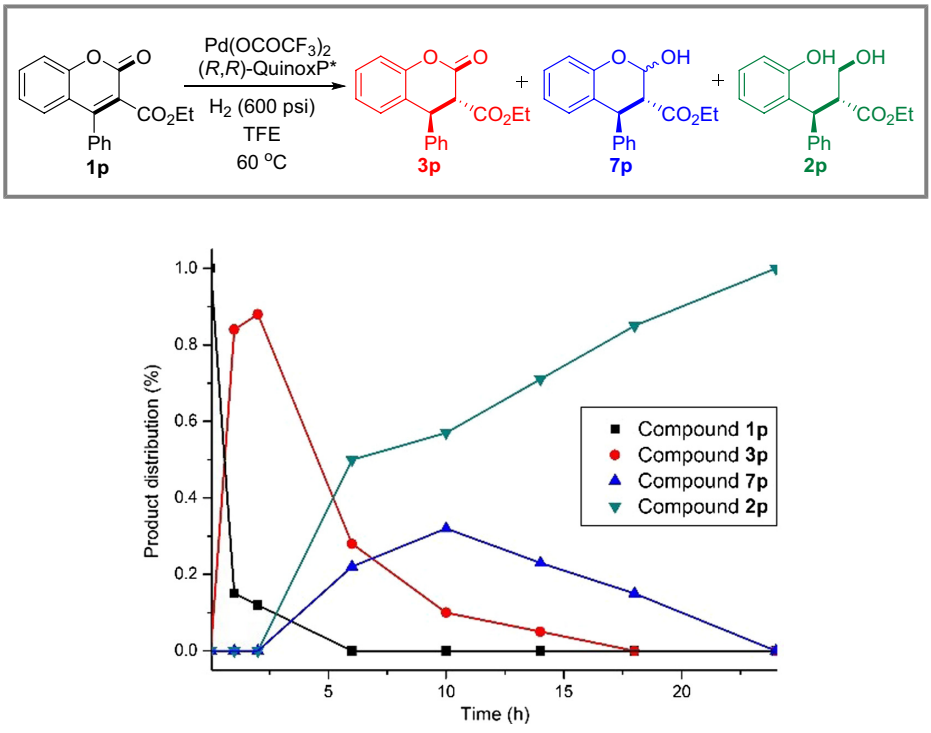

Figure 1 | *Plot of reaction components.*

DOI: 10.31635/ccschem.023.202303564
Citation: *CCS Chem.* **2024**, 6, 1987–1999
Link to VoR: https://doi.org/10.31635/ccschem.023.202303564

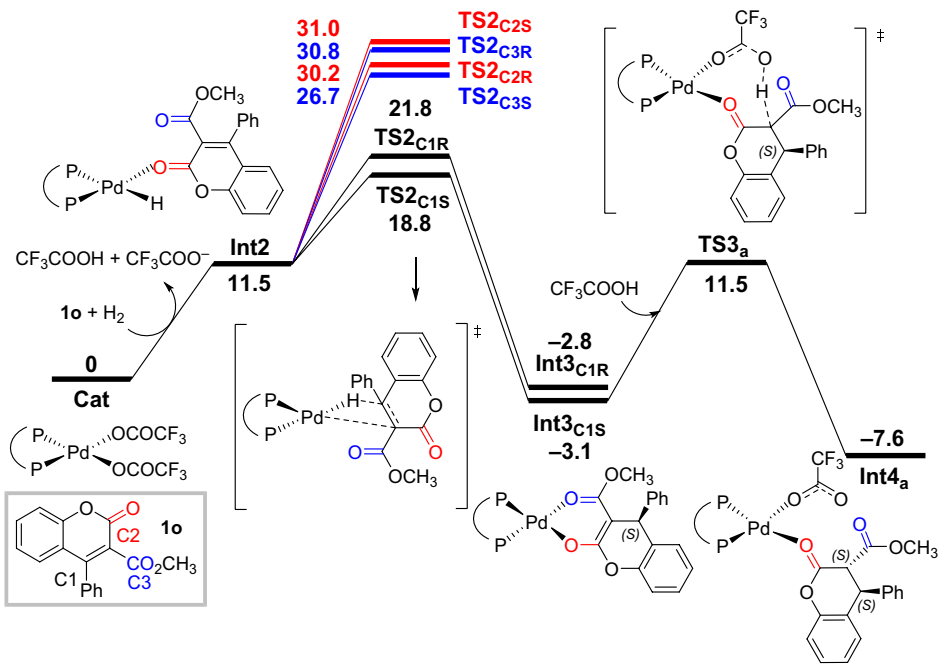

Figure 2 | *Gibbs energy diagram (in kcal/mol) for the first hydrogenation.*

carbon center, and thus six different transition states (Supporting Information Figure S4) were located. The attack on C1 was energetically much more favourable than those on C2 or C3. The total barrier was 18.8 kcal/mol (Figure 2) for the *S* attack **TS2$_{C1S}$**, while it was 3.0 kcal/mol higher for the *R* attack, giving a calculated ee value of higher than 99%. Distortion/interaction analysis[51] on **TS2$_{C1S}$** and **TS2$_{C1R}$** (Supporting Information Figure S9) showed that the distortion energy for the *S* attack was 2.8 kcal/mol smaller than that for the *R* attack, suggesting that the selectivity was mainly distortion-controlled. The steric contour map proposed by the Cavallo group[52] was used to analyze the local environment for the reaction center in the Pd-H catalyst

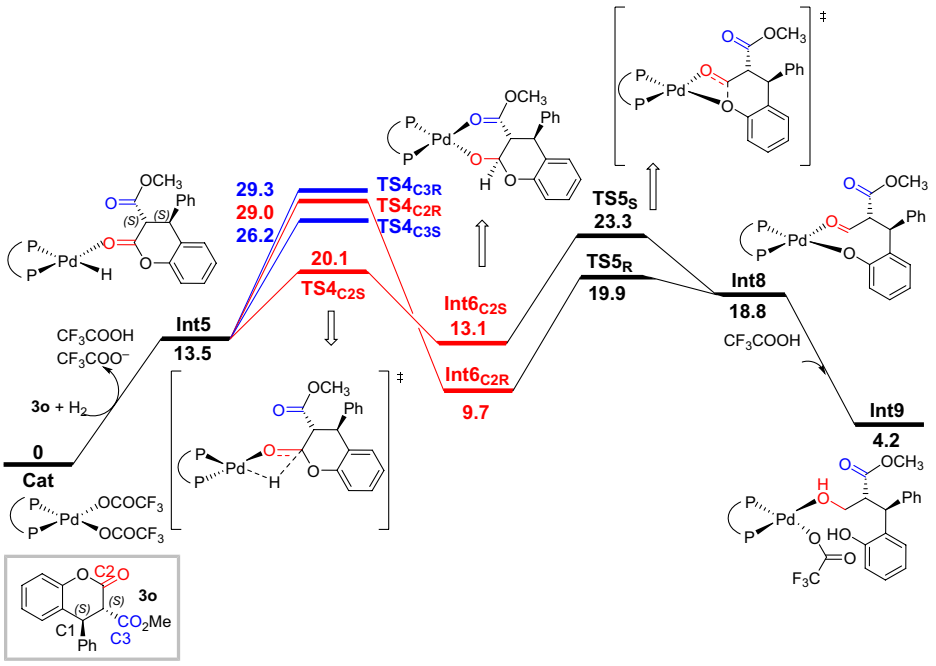

Figure 3 | *Gibbs energy diagram (in kcal/mol) for the second hydrogenation.*

DOI: 10.31635/ccschem.023.202303564
Citation: *CCS Chem.* **2024**, 6, 1987–1999
Link to VoR: https://doi.org/10.31635/ccschem.023.202303564

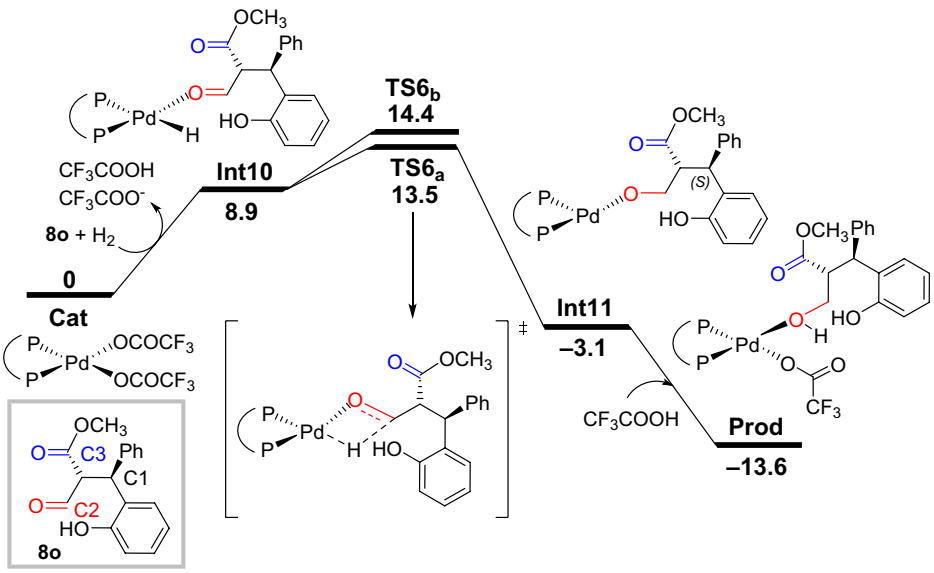

Figure 4 | *Gibbs energy diagram (in kcal/mol) for the third hydrogenation.*

(Supporting Information Figure S11). In **TS2$_{C1S}$**, the C1-attached phenyl ring was located in the less buried zones, which accommodated the substrate better. Further protonation of the α-carbon by CF_3CO_2H was very facile, affording the C=C hydrogenation product **3o**.

Similarly, the hydrogenation of **3o** took place from **Int5**, and the Pd-H species attacked either C2 or C3. Notably, the C2 attack on the lactone carbonyl carbon (**TS4$_{C2S}$**) was preferred due to the lack of steric repulsion between the metal and the phenyl groups, which were in *trans* configuration. Alternatively, the metal and the terminal ester methyl group in **TS4$_{C3S}$** were in the *cis* configuration. Therefore, its barrier was 6.1 kcal/mol higher. Similar to the first hydrogenation, the distortion/interaction analysis on **TS4$_{C2S}$** and **TS4$_{C2R}$** (Supporting Information Figure S10) suggested that the stereoselectivity was also distortion-controlled. From the hemiacetal intermediate **Int6$_{C2S}$**, C–O bond cleavage (**TS5$_S$**) proceeded with a barrier of 23.3 kcal/mol, which turned out to be rate-limiting for the whole reaction. Meanwhile for the *R* attack, **TS4$_{C2R}$** was the rate-limiting transition state with a barrier of 29.0 kcal/mol. Then, protonation of the phenolate led to the production of compound **8o**. Subsequently, protonation of the phenolate led to the production of compound **8o**. The last hydrogenation on the aldehyde carbonyl group was very efficient, with a barrier of only 13.5 kcal/mol (Figure 4).

By comparing the Gibbs energy diagrams for all three hydrogenation processes, it can be seen that the second hydrogenation (Supporting Information Figure S13) has

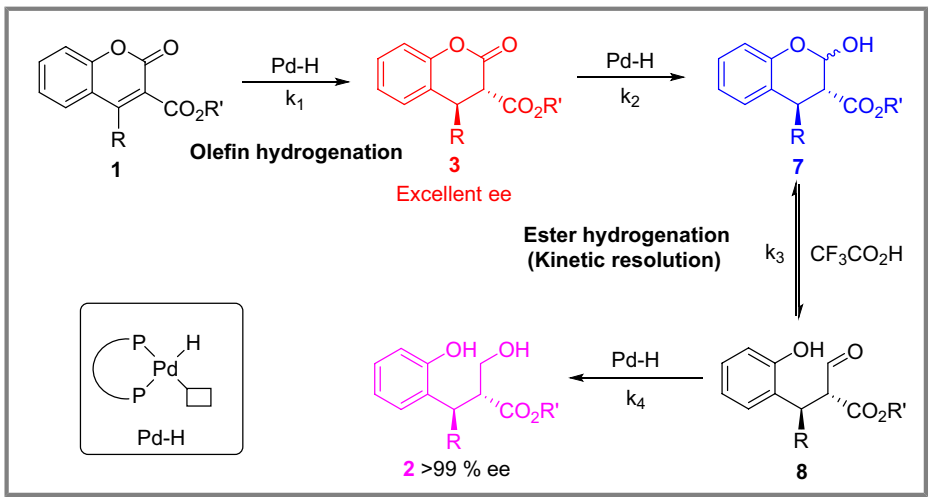

Scheme 6 | *Proposed reaction pathway.*

DOI: 10.31635/ccschem.023.202303564
Citation: *CCS Chem.* **2024**, 6, 1987–1999
Link to VoR: https://doi.org/10.31635/ccschem.023.202303564

the highest barrier, followed by the first one (Supporting Information Figure S12), while the third one is the most efficient. These results corroborate the kinetic data shown in Figure 1, which shows the accumulation of **3p** during the reaction.

Based on the above mechanistic investigation, the asymmetric ATC hydrogenation reaction pathway is proposed in Scheme 6. Firstly, the C=C bond of the α,β-unsaturated lactones **1** is hydrogenated to give the intermediate **3** with high enantioselectivity. Then, the favored isomer is further hydrogenated to afford the intermediate hemiacetal **7** with the same palladium catalyst. Then, trifluoroacetic acid, which can be in situ generated in a palladium catalytic system, catalyzes the elimination of hemiacetal **7** to afford the aldehyde **8**. Finally, due to the high reactivity of aldehyde, the aldehyde **8** is rapidly hydrogenated to yield the target product **2**, and this hydrogenation effectively prevents the racemization of the stereogenic carbon adjacent to the ester functional group. Depending on the distribution of reaction intermediates and the mechanistic studies, the comparison of the reaction rate constants at each step is $k_3 < k_1 \approx k_2 < k_4$. The reaction profile of the four components is shown in Supporting Information.

Conclusion

In conclusion, we have successfully developed an unprecedented palladium-catalyzed asymmetric autotandem hydrogenation of α,β-unsaturated lactones. In this reaction, the C=C bond of α,β-unsaturated lactones are first hydrogenated, giving the chiral dihydrocoumarins with high enantioselectivity. Then, the ester group is further hydrogenated using the same catalytic system. Decreasing the reaction temperature, hydrogenation of the single C=C bond is conveniently carried out, delivering the dihydrocoumarin products with high yield and enantioselectivity. Notably, this is the first time that the homogeneous palladium catalyst has been successfully applied in the hydrogenation of esters under the neutral condition. The above hydrogenation proceeds smoothly on the gram scale, and the products are transformed into useful chiral building blocks without loss of optical purity. In addition, light has also been shed on the reaction mechanism according to the control experiments and DFT calculations. The palladium-catalyzed asymmetric hydrogenation of readily available ester derivatives through dynamic kinetic resolution and kinetic resolution is ongoing in our laboratory.

Footnotes

[a] The ee of **3a** in Table 1 comes from **3a**′.
[b] See the computational section in Supporting Information.

Supporting Information

Supporting Information is available and includes the experimental procedures and characterization of the compounds.

Conflict of Interest

There is no conflict of interest to report.

Funding Information

We thank the National Natural Science Foundation of China (grant no. 22171260), the K.C. Wong Education Foundation (grant no. GJTD-2020-08), and the Bureau of Science and Technology (grant no. XLYC2002080) of Liaoning Province for financial support.

References

1. Anastas, P. T.; Kirchhoff, M. M. Origins, Current Status, and Future Challenges of Green Chemistry. *Acc. Chem. Res.* **2002**, *35*, 686–694.
2. Sheldon, R. A. Fundamentals of Green Chemistry: Efficiency in Reaction Design. *Chem. Soc. Rev.* **2012**, *41*, 1437–1451.
3. Horváth, I. T. Introduction: Sustainable Chemistry. *Chem. Rev.* **2018**, *118*, 369–371.
4. Fogg, D. E.; dos Santos, E. N. Tandem Catalysis: A Taxonomy and Illustrative Review. *Coord. Chem. Rev.* **2004**, *248*, 2365–2379.
5. Shindoh, N.; Takemoto, Y.; Takasu, K. Auto-Tandem Catalysis: A Single Catalyst Activating Mechanistically Distinct Reactions in a Single Reactor. *Chem. Eur. J.* **2009**, *15*, 12168–12179.
6. Camp, J. E. Auto-Tandem Catalysis: Activation of Multiple, Mechanistically Distinct Process by a Single Catalyst. *Eur. J. Org. Chem.* **2017**, *2017*, 425–433.
7. Long, J.; Yu, R.; Gao, J.; Fang, X. Access to 1,3-Dinitriles by Enantioselective Auto-Tandem Catalysis: Merging Allylic Cyanation with Asymmetric Hydrocyanation. *Angew. Chem. Int. Ed.* **2020**, *59*, 6785–6789.
8. Zhu, J.-X.; Chen, Z.-C.; Du, W.; Chen, Y.-C. Asymmetric Auto-Tandem Palladium Catalysis for 2,4-Dienyl Carbonates: Ligand-Controlled Divergent Synthesis. *Angew. Chem. Int. Ed.* **2022**, *61*, e202200880.
9. Peters, B. B. C.; Zheng, J.; Krajangsri, S.; Andersson, P. G. Stereoselective Iridium-*N,P*-Catalyzed Double Hydrogenation of Conjugated Enones to Saturated Alcohols. *J. Am. Chem. Soc.* **2022**, *144*, 8734–8740.
10. Zhang, W.; Chi, Y.; Zhang, X. Developing Chiral Ligands for Asymmetric Hydrogenation. *Acc. Chem. Res.* **2007**, *40*, 1278–1290.
11. Etayo, P.; Vidal-Ferran, A. Rhodium-Catalysed Asymmetric Hydrogenation as a Valuable Synthetic Tool for the Preparation of Chiral Drugs. *Chem. Soc. Rev.* **2013**, *42*, 728–754.

DOI: 10.31635/ccschem.023.202303564
Citation: *CCS Chem.* **2024**, 6, 1987–1999
Link to VoR: https://doi.org/10.31635/ccschem.023.202303564

12. Verendel, J. J.; Pàmies, O.; Diéguez, M.; Andersson, P. G. Asymmetric Hydrogenation of Olefins Using Chiral Crabtree-Type Catalysts: Scope and Limitations. *Chem. Rev.* **2014**, *114*, 2130–2169.
13. Seo, C. S. G.; Morris, R. H. Catalytic Homogeneous Asymmetric Hydrogenation: Successes and Opportunities. *Organometallics* **2019**, *38*, 47–65.
14. Wen, J.; Wang, F.; Zhang, X. Asymmetric Hydrogenation Catalyzed by First-Row Transition Metal Complexes. *Chem. Soc. Rev.* **2021**, *50*, 3211–3237.
15. Lückemeier, L.; Pierau, M.; Glorius, F. Asymmetric Arene Hydrogenation: Towards Sustainability and Application. *Chem. Soc. Rev.* **2023**, *52*, 4996–5012.
16. Yang, X.-H.; Yue, H.-T.; Yu, N.; Li, Y.-P.; Xie, J.-H.; Zhou, Q.-L. Iridium-Catalyzed Asymmetric Hydrogenation of Racemic α-Substituted Lactones to Chiral Diols. *Chem. Sci.* **2017**, *8*, 1811–1814.
17. Chen, G.-Q.; Lin, B.-J.; Huang, J.-M.; Zhao, L.-Y.; Chen, Q.-S.; Jia, S.-P.; Yin, Q.; Zhang, X. Design and Synthesis of Chiral *oxa*-Spirocyclic Ligands for Ir-Catalyzed Direct Asymmetric Reduction of Bringmann's Lactones with Molecular H_2. *J. Am. Chem. Soc.* **2018**, *140*, 8064–8068.
18. Gu, X.-S.; Xiong, Y.; Yang, F.; Yu, N.; Yan, P.-C.; Xie, J.-H.; Zhou, Q.-L. Enantioselective Hydrogenation Toward Chiral 3-Aryloxy Tetrahydrofurans Enabled by Spiro Ir-PNN Catalysts Containing an Unusual 5-Substituted Chiral Oxazoline Unit. *ACS Catal.* **2022**, *12*, 2206–2211.
19. Ito, M.; Ootsuka, T.; Watari, R.; Shiibashi, A.; Himizu, A.; Ikariya, T. Catalytic Hydrogenation of Carboxamides and Esters by Well-Defined Cp*Ru Complexes Bearing a Protic Amine Ligand. *J. Am. Chem. Soc.* **2011**, *133*, 4240–4242.
20. Liu, C.; Xie, J.-H.; Li, Y.-L.; Chen, J.-Q.; Zhou, Q.-L. Asymmetric Hydrogenation of α,α'-Disubstituted Cycloketones Through Dynamic Kinetic Resolution: An Efficient Construction of Chiral Diols with Three Contiguous Stereocenters. *Angew. Chem. Int. Ed.* **2013**, *52*, 593–596.
21. Tan, X.; Wang, Q.; Liu, Y.; Wang, F.; Lv, H.; Zhang, X. A New Designed Hydrazine Group-Containing Ruthenium Complex Used for Catalytic Hydrogenation of Esters. *Chem. Commun.* **2015**, *51*, 12193–12196.
22. Arai, N.; Namba, T.; Kawaguchi, K.; Matsumoto, Y.; Ohkuma, T. Chemoselectivity Control in the Asymmetric Hydrogenation of γ- and δ-Keto Esters into Hydroxy Esters or Diols. *Angew. Chem. Int. Ed.* **2018**, *57*, 1386–1389.
23. Huang, Y.; Berthiol, F.; Stegink, B.; Pollard, M. M.; Minnaard, A. J. Asymmetric Hydrogenation of α,β-Unsaturated Ester-Phosphonates. *Adv. Synth. Catal.* **2009**, *351*, 1423–1430.
24. Sun, H. L.; Chen, F.; Xie, M. S.; Guo, H. M.; Qu, G. R.; He, Y. M.; Fan, Q. H. Asymmetric Hydrogenation of α-Purine Nucleobase-Substituted Acrylates with Rhodium Diphosphine Complexes: Access to Tenofovir Analogues. *Org. Lett.* **2016**, *18*, 2260–2263.
25. Wen, J.; Jiang, J.; Zhang, X. Rhodium-Catalyzed Asymmetric Hydrogenation of α,β-Unsaturated Carbonyl Compounds via Thiourea Hydrogen Bonding. *Org. Lett.* **2016**, *18*, 4451–4453.
26. Li, X.; You, C.; Yang, Y.; Yang, Y.; Li, P.; Gu, G.; Chung, L. W.; Lv, H.; Zhang, X. Rhodium-Catalyzed Asymmetric Hydrogenation of β-Cyanocinnamic Esters with the Assistance of a Single Hydrogen Bond in a Precise Position. *Chem. Sci.* **2018**, *9*, 1919–1924.
27. Liu, G.; Li, A.; Qin, X.; Han, Z.; Dong, X. Q.; Zhang, X. Efficient Access to Chiral β-Borylated Carboxylic Esters via Rh-Catalyzed Hydrogenation. *Adv. Synth. Catal.* **2019**, *361*, 2844–2848.
28. Woodmansee, D. H.; Müller, M.-A.; Neuburger, M.; Pfaltz, A. Chiral Pyridyl Phosphinites with Large Aryl Substituents as Efficient Ligands for the Asymmetric Iridium-Catalyzed Hydrogenation of Difficult Substrates. *Chem. Sci.* **2010**, *1*, 72–78.
29. Li, J. Q.; Quan, X.; Andersson, P. G. Highly Enantioselective Iridium-Catalyzed Hydrogenation of α,β-Unsaturated Esters. *Chem. Eur. J.* **2012**, *18*, 10609–10616.
30. Margalef, J.; Biosca, M.; Cruz-Sánchez, P.; Caldentey, X.; Rodríguez-Escrich, C.; Pàmies, O.; Pericàs, M. A.; Diéguez, M. Indene Derived Phosphorus-Thioether Ligands for the Ir-Catalyzed Asymmetric Hydrogenation of Olefins with Diverse Substitution Patterns and Different Functional Groups. *Adv. Synth. Catal.* **2021**, *363*, 4561–4574.
31. Shevlin, M.; Friedfeld, M. R.; Sheng, H.; Pierson, N. A.; Hoyt, J. M.; Campeau, L. C.; Chirik, P. J. Nickel-Catalyzed Asymmetric Alkene Hydrogenation of α,β-Unsaturated Esters: High-Throughput Experimentation-Enabled Reaction Discovery, Optimization, and Mechanistic Elucidation. *J. Am. Chem. Soc.* **2016**, *138*, 3562–3569.
32. Han, Z.; Liu, G.; Zhang, X.; Li, A.; Dong, X. Q.; Zhang, X. Synthesis of Chiral β-Borylated Carboxylic Esters *via* Nickel-Catalyzed Asymmetric Hydrogenation. *Org. Lett.* **2019**, *21*, 3923–3926.
33. Zhang, Z.; Butt, N. A.; Zhou, M.; Liu, D.; Zhang, W. Asymmetric Transfer and Pressure Hydrogenation with Earth-Abundant Transition Metal Catalysts. *Chin. J. Chem.* **2018**, *36*, 443–454, and references cited therein.
34. Chen, Q.-A.; Ye, Z.-S.; Duan, Y.; Zhou, Y.-G. Homogeneous Palladium-Catalyzed Asymmetric Hydrogenation. *Chem. Soc. Rev.* **2013**, *42*, 497–511, and references cited therein.
35. Feng, G.-S.; Chen, M.-W.; Shi, L.; Zhou, Y.-G. Facile Synthesis of Chiral Cyclic Ureas Through Hydrogenation of 2-Hydroxypyrimidine/Pyrimidin-2(1*H*)-One Tautomers. *Angew. Chem. Int. Ed.* **2018**, *57*, 5853–5857.
36. Chen, J.; Zhang, Z.; Li, B.; Li, F.; Wang, Y.; Zhao, M.; Gridnev, I. D.; Imamoto, T.; Zhang, W. $Pd(OAc)_2$-Catalyzed Asymmetric Hydrogenation of Sterically Hindered *N*-Tosylimines. *Nat. Commun.* **2018**, *9*, 5000–5009.
37. Shen, G.; Chen, J.; Xu, D.; Zhang, X.; Zhou, Y.; Fan, B. Asymmetric Transfer Hydrogenation of Heterobicyclic Alkenes with Water as Hydrogen Source. *Org. Lett.* **2019**, *21*, 1364–1367.
38. Feng, S.; Tang, Y.; Yang, C.; Shen, C.; Dong, K. Synthesis of Enantioenriched α,α-Difluoro-β-Arylbutanoic Esters by Pd-catalyzed Asymmetric Hydrogenation. *Org. Lett.* **2020**, *22*, 7508–7512.

DOI: 10.31635/ccschem.023.202303564
Citation: *CCS Chem.* **2024**, 6, 1987–1999
Link to VoR: https://doi.org/10.31635/ccschem.023.202303564

39. Yu, C.-B.; Wang, H.-D.; Song, B.; Shen, H.-Q.; Fan, H.-J.; Zhou, Y.-G. Reversal of Diastereoselectivity in Palladium-Arene Interaction Directed Hydrogenative Desymmetrization of 1,3-Diketones. *Sci. China Chem.* **2020**, *63*, 215–221.
40. Kraft, S.; Ryan, K.; Kargbo, R. B. Recent Advances in Asymmetric Hydrogenation of Tetrasubstituted Olefins. *J. Am. Chem. Soc.* **2017**, *139*, 11630–11641.
41. Cui, X.; Burgess, K. Catalytic Homogeneous Asymmetric Hydrogenations of Largely Unfunctionalized Alkenes. *Chem. Rev.* **2005**, *105*, 3272–3296.
42. Schrems, M. G.; Neumann, E.; Pfaltz, A. Iridium-Catalyzed Asymmetric Hydrogenation of Unfunctionalized Tetrasubstituted Olefins. *Angew. Chem. Int. Ed.* **2007**, *46*, 8274–8276.
43. Wang, Q.; Huang, W.; Yuan, H.; Cai, Q.; Chen, L.; Lv, H.; Zhang, X. Rhodium-Catalyzed Enantioselective Hydrogenation of Tetrasubstituted α-Acetoxy β-Enamido Esters: A New Approach to Chiral α-Hydroxyl-β-amino Acid Derivatives. *J. Am. Chem. Soc.* **2014**, *136*, 16120–16123.
44. Liu, Y.-T.; Chen, J.-Q.; Li, L.-P.; Shao, X.-Y.; Xie, J.-H.; Zhou, Q.-L. Asymmetric Hydrogenation of Tetrasubstituted Cyclic Enones to Chiral Cycloalkanols with Three Contiguous Stereocenters. *Org. Lett.* **2017**, *19*, 3231–3234.
45. Wang, J.; Zhu, Z.-H.; Chen, M.-W.; Chen, Q.-A.; Zhou, Y.-G. Catalytic Biomimetic Asymmetric Reduction of Alkenes and Imines Enabled by Chiral and Regenerable NAD(P)H Models. *Angew. Chem. Int. Ed.* **2019**, *58*, 1813–1817.
46. Zhu, Z.-H.; Ding, Y.-X.; Wu, B.; Zhou, Y.-G. Design and Synthesis of Chiral and Regenerable [2.2]Paracyclophane-Based NAD(P)H Models and Application in Biomimetic Reduction of Flavonoids. *Chem. Sci.* **2020**, *11*, 10220–10224.
47. Zhao, Q.-K.; Wu, X.; Yang, F.; Yan, P.-C.; Xie, J.-H.; Zhou, Q.-L. Catalytic Asymmetric Hydrogenation of 3-Ethoxycarbonyl Quinolin-2-Ones and Coumarins. *Org. Lett.* **2021**, *23*, 3593–3598.
48. McGuire, M. A.; Shilcrat, S. C.; Sorenson, E. An Efficient Asymmetric Catalytic Hydrogenation of 4-Aryl Coumarins, Preparation of a Key Intermediate in the Synthesis of a Class of Endothelin Receptor Antagonists. *Tetrahedron Lett.* **1999**, *40*, 3293–3296.
49. Ulgheri, F.; Marchetti, M.; Piccolo, O. Enantioselective Synthesis of (*S*)- and (*R*)-Tolterodine by Asymmetric Hydrogenation of a Coumarin Derivative Obtained by a Heck Reaction. *J. Org. Chem.* **2007**, *72*, 6056–6059.
50. Xu, Y.; Liu, D.; Deng, Y.; Zhou, Y.; Zhang, W. Rhodium-Catalyzed Asymmetric Hydrogenation of 3-Benzoylaminocoumarins for the Synthesis of Chiral 3-Amino Dihydrocoumarins. *Angew. Chem. Int. Ed.* **2021**, *60*, 23602–23607.
51. Fernandez, I.; Bickelhaupt, F. M. The Activation Strain Model and Molecular Orbital Theory: Understanding and Designing Chemical Reactions. *Chem. Soc. Rev.* **2014**, *43*, 4953–4967, and references cited therein.
52. Falivene, L.; Cao, Z.; Petta, A.; Serra, L.; Poater, A.; Oliva, R.; Scarano, V.; Cavallo, L. Towards the Online Computer-Aided Design of Catalytic Pockets. *Nat. Chem.* **2019**, *11*, 872–879.

DOI: 10.31635/ccschem.023.202303564
Citation: *CCS Chem.* **2024**, 6, 1987–1999
Link to VoR: https://doi.org/10.31635/ccschem.023.202303564